PREPRINT

GADMA2: more efficient and flexible demographic inference from genetic data

Ekaterina Noskova[1,*], Nikita Abramov[2], Stanislav Iliutkin[1], Anton Sidorin[3], Pavel Dobrynin[1,4,†] and Vladimir Ulyantsev[1,†]

[1]Computer Technologies Laboratory, ITMO University, St. Petersburg, 197101, Russia and [2]HSE University, St. Petersburg, 194100, Russia and [3]Laboratory of Biochemical Genetics, St. Petersburg State University, St. Petersburg, 199034, Russia and [4]Human Genetics Laboratory, Vavilov Institute of General Genetics RAS, Moscow, 119991, Russia

[*]ekaterina.e.noskova@gmail.com
[†]Denotes shared senior authorship, listed alphabetically.

Abstract

Background: Inference of complex demographic histories is a source of information about events that happened in the past of studied populations. Existing methods for demographic inference typically require input from the researcher in the form of a parameterized model. With an increased variety of methods and tools, each with its own interface, the model specification becomes tedious and error-prone. Moreover, optimization algorithms used to find model parameters sometimes turn out to be inefficient. The open-source software GADMA addresses these problems, providing automatic demographic inference. It proposes a common interface for several inference engines and provides global parameters optimization based on a genetic algorithm.
Results: Here, we introduce the new GADMA2 software and provide a detailed description of the added and expanded features. It has a renovated core code base, new inference engines, an updated optimization algorithm and a flexible setup for automatic model construction. We provide a full overview of GADMA2 enhancements, compare the performance of supported inference engines on simulated data and demonstrate an example of GADMA2 usage on two empirical datasets.
Conclusions: We demonstrate the better performance of a genetic algorithm in GADMA2 by comparing it to the initial version and other existing optimization approaches. Our experiments on simulated data indicate that GADMA2's inference engines are able to provide accurate estimations of demographic parameters even for misspecified models. We improve model parameters for two empirical datasets of inbred species.

Key words: demographic inference; population genetics; genetic algorithm; hyperparameter optimization.

Introduction

The evolutionary forces form a genetic variety of closely-related species and populations. Principal historical events like divergence, population size change, migration and selection could be reconstructed from the genetic data using different algorithmic and statistical approaches. Inference of complex demographic histories is widely applied in conservation biology studies to identify major events in the population's past. It supplements archaeological information about the historical processes that have left no paleontological records. Finally, demographic histories form the basis for subsequent population studies and medical genetic research.

In recent years many methods for demographic inference have appeared to investigate the demographic histories of species or populations [1, 2, 3, 4, 5, 6]. Most of them consist of two somewhat independent components. The first component provides means to compute data statistics under a proposed demographic history and compare them with real data by the log-likelihood value. One of the most widely-used data statistics is the allele frequency spectrum (e.g., [1, 2, 4]). However, newer methods based on two-locus [7] and linkage disequilibrium (LD) statistics [8, 9] have also become available. This paper will denote the first component as an *infer-*

Compiled on: October 12, 2022.
Draft manuscript prepared by the author.

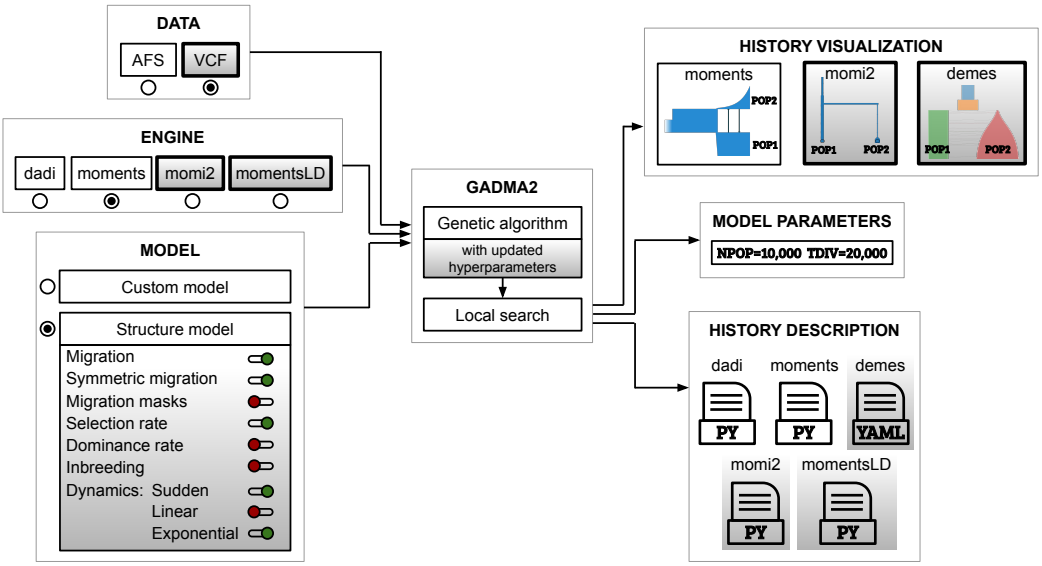

Figure 1. Scheme of GADMA2. New features and enhancements are marked with a gradient grey colour. GADMA2 takes input genetic data presented in either AFS or VCF formats, engine name and model specifications and provides inferred model parameters, visualization and descriptions of the final demographic history.

ence engine. The second component of existing tools is *optimization*. It requires a user-defined model of demographic history and performs a search of the maximal likelihood model parameters using different optimization algorithms. While a number of optimization techniques are provided, they often turn out to be ineffective in practical applications [10].

In 2020 we presented a new software GADMA [10] for unsupervised demographic inference from the allele frequency spectrum (AFS) data. GADMA separates two regular components. It provides a common interface for various already existing inference engines and introduces new global search optimization based on a genetic algorithm. GADMA does not require model specification. Instead, it takes *model structure* that determines how many time epochs are included in the model. Previously, models of demographic history were parameterized only by continuous parameters and had fixed population size dynamics. Constant size or exponential growth could be examples of such dynamics. GADMA's model with structure extends the regular concept of a model by including dynamics as discrete model parameters. Thus, it can automatically construct history as a sequence of time epochs with desired parameter types from blocks of constant, linear and exponential size changes. The researcher has control over the types of model parameters to infer, for example, all migrations could be disabled. It was shown that the proposed genetic algorithm approach in GADMA has better performance than previously existing optimization algorithms both on simulated and real datasets [10]. Since its initial publication, GADMA has been applied in several studies on a variety of species: Xiong et al. [11], Valdez and D'Elía [12], Pazhenkova and Lukhtanov [13], Cassin-Sackett et al. [14], Buggiotti et al. [15].

The initial version of GADMA features only two inference engines: ∂a∂i [1] and *moments* [2]. Both of these engines compute the allele frequency spectrum statistics using Wright-Fisher diffusion-based approach and, thus, provide similar results. Among the variety of other available tools, we can highlight methods based either on AFS (*momi2*, *fastsimcoal2*), LD statistics (*momentsLD*), or haplotype data (diCal2) as potential additions to the supported engines in GADMA. Some already implemented features of ∂a∂i and *moments*, like the inference of selection and dominance rates, are not included in the first version of GADMA. Both ∂a∂i and *moments* have been upgraded since these programs were first published and since GADMA's initial release. For example, ∂a∂i introduced inference of the inbreeding coefficients [16], started to support demographic histories involving four and five populations and enabled GPU support [17]. In light of these advancements, we have sought to extend GADMA in several directions to support new features and engines and further enhance its optimization algorithm.

In this paper, we describe new capabilities implemented in GADMA2. We compare supported inference engines of GADMA2 on two simulated datasets for different demographic models. Furthermore, we demonstrate the efficiency of the updated version on two empirical datasets of inbred species from Blischak et al. [16].

GADMA2 has an updated core codebase and implements a more efficient and flexible unsupervised demographic inference method. The improved version extends the initial GADMA in several ways (Figure 1). First, the genetic algorithm in GADMA2 is improved by hyperparameter optimization. New values of the genetic algorithm hyperparameters that provide more efficient and stable convergence are found. Second, GADMA2 provides more flexible control of the model specification for automatic model construction. For example, it is possible to include inferences about selection and inbreeding coefficients. Third, two new inference engines are integrated: *momi2* and *momentsLD*. Thus, GADMA2 supports four engines overall. Lastly, several functional enhancements are integrated, including the ability to use data in VCF format and new engines for history representation and visualization (*momi2* and *demes*).

Materials and methods

Datasets

We use several datasets in this work. Datasets for the hyperparameter optimization are taken from the Python package `deminf_data v1.0.0` (Figure S1) that is available on GitHub via the link: https://github.com/noscode/demographic_inference_data. `Deminf_data` contains various datasets with both real and simulated AFS data. Simulations are performed with *moments* [2] software. Each dataset is named according to the convention described in Figure S1 and includes a) the allele frequency spectrum data; b) the model of the demographic history; and c) bounds of the model parameters. Full descriptions of the data and demographic model parameters of datasets are available in the repository on GitHub. For hyperparameter optimization we used ten datasets from `deminf_data`: four as training problem instances and six for testing. Basic descriptions of these datasets are available in sec-

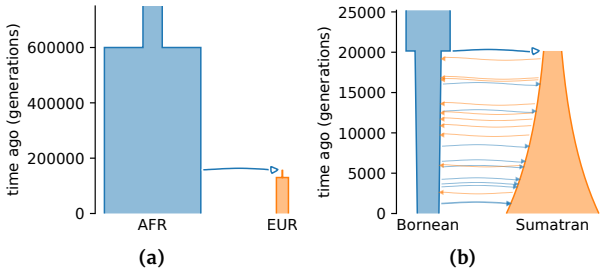

Figure 2. Demographic histories used in data simulations powered by *stdpopsim* [18] for performance comparison of GADMA2 inference engines. (a) History of African (AFR) and European (EUR) populations of *Drosophila melanogaster* from Li and Stephan [19]. (b) History of *Pongo pygmaeus* (Bornean) and *Pongo abelii* (Sumatran) orangutan species from Locke et al. [20].

tion S1.1 of Supplementary Materials.

The performance of GADMA2's engines is evaluated on two simulated datasets: populations of fruit flies and orangutan species. For simulation purposes we used a previously described scenarios available within the *stdpopsim* library [18]. Each dataset simulated by *msprime* engine [21] includes genetic data of five diploid individuals per each population.

Li and Stephan [19] presented the demographic history of *Drosophila melanogaster* populations from Africa and Europe. The visual representation of the history is shown in Figure 2a. The African population is characterized by a single instantaneous expansion. The origin of the European population is a result of the divergence of a very limited number of individuals followed by instantaneous expansion. Five autosomal chromosomes with a total length of 0.11 Gbp are simulated under this demographic history. We use mutation rate equal to $5.49 \cdot 10^{-9}$ per base per generation [22] and recombination rate of $8.4 \cdot 10^{-9}$ per base per generation [23].

The demographic history of the Bornean (*Pongo pygmaeus*) and Sumatran (*Pongo abelii*) orangutans was originally inferred in Locke et al. [20] and is shown on Figure 2b. Specifically, it is an isolation-with-migration history that describes the ancestral population split followed by the exponential growth of Sumatran and an exponential decline of Bornean orangutans. We simulate 23 autosomal chromosomes with a total length of 2.87 Gbp. The mutation rate used in the simulation is equal to $1.5 \cdot 10^{-8}$ per site per generation [24]. Averaged recombination rates for each chromosome are taken from the *Pongo abelii* recombination map inferred in Nater et al. [24].

Datasets for the demographic inference of inbred species are taken from the original paper Blischak et al. [16]. The 11×5 AFS data for two populations of the American puma (*Puma concolor*) was constructed on the basis of Ochoa et al. [25]. The AFS data for 45 individuals of domesticated cabbage (*Brassica oleracea*) was obtained from publicly available resequencing data [26, 27]. Both allele frequency spectra are folded due to a lack of information about ancestral alleles. Datasets are presented in the repository of the original article and are available via the following link: `https://github.com/pblischak/inbreeding-sfs`.

Hyperparameter optimization

GADMA uses a genetic algorithm to optimize the demographic parameters [10]. A *hyperparameter* is usually defined as a parameter of an algorithm. The performance of any algorithm depends on its hyperparameters, and optimization of their values can significantly improve the overall efficiency. As an example of a hyperparameter, we can consider the number of demographic models in one iteration of the genetic algorithm. Several techniques can be used for the optimization of hyperparameters, and Bayesian optimization is a primary method among them [28]. The most popular and efficient method based on the Bayesian optimization that performs hyperparameter optimization on the proposed set of problem instances is implemented in SMAC software [29, 30]. It has been applied in a number of studies including optimization of neural networks [31, 32, 33].

We use SMAC to tune the hyperparameters of the genetic algorithm in GADMA2. The descriptions and domains of all hyperparameters are available in Table S1 and Table S2 correspondingly. We perform several attempts of SMAC optimization for different configurations of hyperparameters. First, optimization of all genetic algorithm hyperparameters is executed. Then two discrete hyperparameters (`gen_size` and `n_init_const`) are fixed to five manually picked combinations of domain values. SMAC is used to find optimal continuous hyperparameters for each combination. Four combinations were excluded from the analysis. Hyperparameter `gen_size` that corresponds to the size of generation in a genetic algorithm is not tested for the value of 100 due to relatively slow convergence. That eliminate three combinations. Additionally, the constant of initial design `n_init_const` equal to 5 is excluded for a case of `gen_size` equal to 50 as it provides a small number of solutions for the first generation.

Overall, six attempts of hyperparameter optimization using SMAC are made. The optimization is performed for GADMA's genetic algorithm using *moments* engine and four datasets as training problem instances. Each attempt is running for two weeks, in parallel on 10 processes (Intel® Xeon® Gold 6248). In order to achieve a valid comparison within the SMAC framework, GADMA runs are stopped after a fixed number of likelihood evaluations. We take $200 \times$ number of parameters as the stop criteria for the genetic algorithm runs in SMAC. Such a number of evaluations is a trade-off between speed and accuracy: according to the convergence plots, the convergence of default genetic algorithm optimization is slowing down at this point and is very close to the plateau walk (Figure S2, Figure S3). The final configurations are compared for AFS-based engines (*moments*, ∂a∂i and *momi2*) by the SMAC scores evaluated independently from 128 runs on four training and additional six test datasets. More information and details are available in section S1 of Supplementary Materials.

Performance test of GADMA2 engines

Four engines supported by GADMA2 (∂a∂i, *moments*, *momi2*, *momentsLD*) are compared on two simulated datasets of fruit fly populations and orangutan species. For each dataset we test several models of the demographic history. The first two models are based on the ground truth history used in the simulations but differ in the presence of migration. Then we infer parameters for two structure models with and without migration using the GADMA2 feature for automatic demographic inference. For the orangutan dataset three additional models with pulse migrations are analyzed. The performance of all four engines is compared, however, *momi2* engine is not tested for models with continuous migration as it does not support it. We run GADMA2 inference eight times for each engine and model. Parameters of the history with the best log-likelihood are reported. Mutation and recombination rates for demographic inference are taken the same as in the data simulation. Their values are available in Datasets section.

Using GADMA2 engines we find and compare parameters for four models of *Drosophila melanogaster* demographic history (Table S6). Model DROS-NOMIG is an isolation model with instantaneous size change of the African population followed by separation of the European population which experiences two epochs of constant sizes. Population sizes during these epochs are not dependent with each other. Model DROS-MIG describes the identical to DROS-NOMIG scenario but includes continuous asymmetric migration between populations from their divergence till presence. Both models DROS-NOMIG and DROS-MIG align with the original isolation history used for data simulation. Lastly, we test two models with (DROS-STRUCT-MIG) and without (ROS-STRUCT-

NOMIG) migration for structure (2, 1). This notation could be read as a model consisting of two epochs before the ancestral population split followed by divergence and one epoch for each of the two subpopulations. More details on model structure specification can be found in Noskova et al. [10]. By their definition, these structure models are misspecified due to simplification of the European population's history: a two-epoch scenario of the European population is approximated by one epoch with either constant size, linear or exponential change.

We analyze engines' performance on the orangutan dataset for seven demographic models (Table S14). Model ORAN-NOMIG is isolation with the ancestral population split followed by the exponential size changes of the Sumatran and Bornean orangutans. Model ORAN-MIG aligns with the history used in data simulation and describes an isolation-with-migration with the ancestral population split followed by the exponential size changes of the Sumatran and Bornean orangutans. Additional two models with structure (1, 1) without (ORAN-STRUCT-NOMIG) and with continuous migration (ORAN-STRUCT-MIG) are included in the analysis. We note that the original history contains gene flow and can be correctly estimated using ORAN-MIG and ORAN-STRUCT-MIG models.

In order to overcome *momi2*'s limitation on continuous migrations presented in the orangutan history, we tested the engine for additional demographic scenarios with pulse migrations. A different number of pulse migrations with equal rates are uniformly distributed within the epoch between the present time and species divergence time. ORAN-NOMIG model is compared with three additional demographic models: 1) with one pulse migration (ORAN-PULSE1), 2) with three pulse migrations (ORAN-PULSE3), and 3) with seven pulse migrations (ORAN-PULSE7).

Inference of inbreeding coefficients

We perform demographic inference with GADMA2 using the data of the American pumas (*Puma concolor*) and domesticated cabbage (*Brassica oleracea* var. *capitata*) from Blischak et al. [16]. For each dataset parameters of two demographic models are inferred: 1) model from the original paper without inbreeding; 2) model from the original paper with inbreeding. Each demographic inference is run 100 times, and the history with the highest log-likelihood value is selected. Two result histories are compared with the likelihood ratio test [34] to investigate which history best fits the data.

First, we use the same parameter bounds to repeat the demographic inference from Blischak et al. [16] with GADMA2. We compare the results of 100 runs of GADMA2 with the same number of results received in Blischak et al. [16] using ∂a∂i's optimization techniques. Then we perform another round of demographic inference with GADMA2 using wider bounds of parameters.

Mutation rates, generation times and sequence lengths for parameter translation were taken from Blischak et al. [16]. Demographic parameters for *Puma concolor* are translated from the genetic to real units using a mutation rate of $\mu = 2.2 \times 10^{-9}$, a generation time of 3 years, and a sequence length of 2,564,692,624 bp [25]. In the case of *Brassica oleracea* var. *capitata* population demographic parameters are translated using mutation rate of $\mu = 1.5 \times 10^{-8}$, a generation time of 1 year, and a sequence length of 411,560,319 bp.

Reported confidence intervals are estimated on 100 bootstrapped AFS data from the original paper using the Godambe information matrix with a step size equal to $\epsilon = 10^{-2}$ [34]. The scripts and data used for CI evaluation are taken from the repository of Blischak et al. [16] article: https://github.com/pblischak/inbreeding-sfs.

Table 1. Values of the genetic algorithm hyperparameters after each optimization attempt with SMAC. Hyperparameter values from attempt 1 are equal to the default GADMA values as SMAC failed to find a better configuration. For each attempt of 2-6 attempts two discrete hyperparameters (`gen_size` and `n_init_const`) are fixed in order to gain SMAC efficiency.

Hyperparameter ID	Attempt number					
	1 (default)	2	3	4	5	6
`gen_size`	10	10*	10*	10*	50*	50*
`n_init_const`	10	10*	5*	20*	10*	20*
`p_elitism`	0.20	0.30	0.30	0.40	0.40	0.40
`p_mutation`	0.30	0.20	0.20	0.10	0.08	0.10
`p_crossover`	0.30	0.30	0.30	0.30	0.42	0.46
`p_random`	0.20	0.20	0.20	0.20	0.10	0.04
`mutation_strength`	0.200	0.776	0.370	0.534	0.833	0.528
`const_mutation_strength`	1.010	1.302	1.290	1.648	1.199	1.492
`mutation_rate`	0.200	0.273	0.886	0.882	0.595	0.345
`const_mutation_rate`	1.020	1.475	1.942	1.417	1.645	1.472

* These values are fixed during the hyperparameter optimization with SMAC.

Results and discussion

Updated genetic algorithm

The genetic algorithm in GADMA2 is improved by the hyperparameter optimization implemented in SMAC software [29, 30]. Ten hyperparameters (Table 1) of the genetic algorithm were optimized during the first optimization attempt. SMAC performed 13,900 runs of the genetic algorithm and tested 2,222 different hyperparameter configurations. This process took two weeks of continuous computations on cluster. However, SMAC failed to find a better solution than the default one. We assume that such behavior may be caused by the presence of two discrete hyperparameters in the configuration. These hyperparameters are fixed to five specific combinations of the domain values during the next attempts of SMAC-based optimization of the remaining continuous hyperparameters.

As a result, we perform six attempts of hyperparameter optimization for different configurations of GADMA2. Final configurations obtained from SMAC are presented in Table 1. The mean SMAC scores for AFS-based engines evaluated from 128 independent runs can be found in Table S3 for the *moments* engine, Table S4 for the ∂a∂i engine and Table S5 for the *momi2* engine. The costs and results for ∂a∂i are very similar to those shown in Table S3 with runs executed using the *moments* engine. These results support the idea that the ∂a∂i and *moments* engines have very similar performance. The convergence plots of a genetic algorithm with different configurations on training and test datasets are presented in Figures S2, S3 for *moments* engine, Figures S4, S5 for ∂a∂i engine and Figures S6, S7 for *momi2* engine.

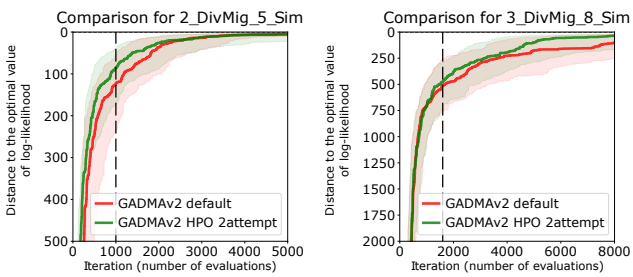

(a) (b)

Figure 3. Example convergence plots for the default genetic algorithm configuration from the initial version of GADMA (red colour) and configuration obtained during attempt 2 of hyperparameter optimization with SMAC (green colour) on two datasets: (a) training dataset `2_DivMig_5_Sim`, (b) test dataset `3_DivMig_8_Sim`. For each configuration 128 independent optimization runs were performed. Solid lines correspond to median convergence over 128 runs and shadowed areas are ranges between the first (0.25) and third (0.75) quartiles. The vertical dashed black line refers to the number of evaluations used to stop a genetic algorithm in SMAC.

Configuration from attempt 2 shows better and faster convergence averaged over all three engines compared to other configurations. Thus, hyperparameters from attempt 2 are chosen as new updated hyperparameters for the genetic algorithm in GADMA2 (Figure 3). However, we note that according to the convergence plots on a greater number of iterations for *moments* engine the configuration from attempt 6 demonstrates better median convergence and better confidence intervals on some datasets (Figure S2 and Figure S3). Configuration from attempt 4 also shows good performance on several datasets both for ∂a∂i and *momi2* engine (Table S4, Table S5 and Figures S4–S7).

Flexible structure model

Automatic demographic model construction is a central feature of GADMA. It replaces the fully manual choice of a model with a *model structure* specification. Traditionally, demographic models only have continuous parameters. Demographic structures, on the other hand, define the number of epochs before, after and between population splitting events and assign a discrete variable representing population dynamics type to each epoch. GADMA optimizes over these discrete variables alongside with the usual continuous ones, examining what would be a multitude of models in the traditional sense. GADMA2 gives the user more control over the search space in this setting.

Migration rates. One of the existing controls over model parameters is the opportunity to disable all migration events and to infer demographic history without any gene flow. GADMA2 now includes a new control handle to make migrations symmetric. Additionally, it allows for specific migrations to be disabled by setting up migration masks.

Selection and dominance rates. Both of the initially supported inference engines included in GADMA, ∂a∂i and *moments*, are able to infer selection and dominance rates. The first version of GADMA lacked the function to make these inferences and we have added these in the new version. GADMA2 enables the approximation of selection rates and dominance coefficients for automatically constructed demographic models.

Population size dynamics. GADMA2 provides additional flexibility for population size estimation during model construction. Previously, demographic parameters such as functions of population size changes were estimated within a fixed set of three possible dynamics: constant, linear, or exponential change. Now, the list of available population size dynamics in GADMA2 can be appointed to any subset of three basic functions. Thus, for example, linear size change can be excluded from the demographic inference if only constant and exponential dynamics are applicable, like in the case of *momi2* engine.

Inbreeding coefficients. Since the publication of the first version of GADMA, the supported inference engines were also upgraded. GADMA2 follows these changes and includes inference of inbreeding coefficients that were implemented in ∂a∂i [16]. Using this new feature included in ∂a∂i, we demonstrate that GADMA2 provides better and more stable results for inference of the demographic models obtained from data for the puma and cabbage reported by Blischak et al. [16] (Figure 4 and Figure S8).

Data formats

Another improvement of ∂a∂i and *moments* is the ability to build an AFS dataset directly from a VCF file. Before this feature was implemented, this had to be done either manually or using another software like *easySFS* (https://github.com/isaacovercast/easySFS). GADMA2 is able to read data directly from a VCF file and downsize, exclude populations from, or build a folded AFS automatically. Such a feature allows broader and more convenient usage of GADMA2.

New inference engines

In addition to ∂a∂i and *moments*, GADMA2 now includes two new inference engines: *momi2* [4] and *momentsLD* [8, 9]. Thus, four engines are provided in the common interface of GADMA2. Both ∂a∂i and *moments* engines are based on the Wright-Fisher diffusion and use allele frequency spectrum statistics for demographic inference.

Momi2 implements a structured coalescent — backward-in-time stochastic process which is dual to the Wright-Fisher diffusion yet scales well to a large number of populations. It also uses AFS data as ∂a∂i and *moments*, but is computationally faster and can handle up to ten populations. However, *momi2* does not support continuous migration and linear change of population size.

Even though the allele frequency spectrum is one of the most popular statistics for demographic inference, it has limitations on how informative it can be [35]. The software *moments* has a submodule *momentsLD* dedicated to demographic inference using linkage disequilibrium (LD) statistics. In general, low-order two-locus LD statistics are used in *momentsLD*. A new inference engine using *momentsLD* is the first engine in GADMA that does not use AFS-based statistics.

Overall, GADMA2 now provides a choice of four inference engines and we encourage the community to extend this list.

A new engine for demographic history representation

During demographic inference GADMA provides different textual and visual representations of the current best demographic history, such as generated Python code for all available inference engines or picture with visualized demographic history. Recently, a new Python package named *demes* [36] appeared to allow standard human-readable descriptions of demographic histories. GADMA2 includes *demes* as an engine to generate native descriptions and plots of demographic histories, which was only possible before using the *moments* or *momi2* engine. Figure 2 shows the examples of visual representations of demographic history using *demes*.

Availability

GADMA2 is freely available from GitHub via the link https://github.com/ctlab/GADMA and can be easily installed via Pip or BioConda. Detailed documentation is located on the website https://gadma.readthedocs.io and includes user-manual, ready-to-use examples, and a section about Application Programming Interface (API). API enables an opportunity to use GADMA2 as a Python package and allows its optimization algorithms to be applied to any general optimization problem. An example of such usage is demonstrated for Rosenbrook function [37] optimization and is provided in the documentation.

The scripts and the results of hyperparameter optimization experiments are saved in the repository and available via the link: https://github.com/noscode/HPO_results_GADMA. The results of GADMA runs for different hyperparameter configurations are stored as an archive available via the link: https://ctlab.itmo.ru/files/papers_files/GADMA2/comparison_on_datasets.zip. The results of experiments about inbreeding are added to the repository with the final demographic histories inferred in the original paper of GADMA and are located via the link: https://bitbucket.org/noscode/gadma_results.

Performance comparison of GADMA2 engines

We compare four inference engines supported by GADMA2 on two simulated datasets of fruit flies and orangutans. Several demographic models are used. Their description is provided in Performance test of GADMA2 engines section of Materials and methods.

The simulated parameter values of *Drosophila melanogaster* population history and their estimations inferred by engines in GADMA2 are presented in Tables 2, S7, S8 and S9 for DROS-NOMIG, DROS-MIG, DROS-STRUCT-NOMIG and DROS-STRUCT-MIG models correspondingly. The mean time of one log-likelihood evaluation and the mean number of evaluations averaged over inference runs are reported in Tables S10 and S11.

Estimations of orangutan history model parameters and their ground truth values are available in Tables S15, S16, S17 and 3 for ORAN-NOMIG, ORAN-MIG, ORAN-STRUCT-NOMIG and ORAN-STRUCT-MIG models respectively. The results of parameter estimations using *momi2* for models with zero, one, three and seven pulse migrations are presented in Table 4. The average time of one log-likelihood evaluation and the mean number of evaluations for used models and engines are reported in Tables S18 and S19.

Below we present our general conclusions about the results. A more detailed comparison is available in section S2 of Supplementary Materials.

Fruit fly demographic history

Parameter values for models DROS-NOMIG and DROS-MIG that align with the ground truth are inferred accurately by all tested inference engines. Best estimations are obtained for the DROS-NOMIG model using *momi2* engine. The bottleneck European population size is approximated most accurately by *momentsLD* engine. Result histories for model DROS-MIG have worse values of log-likelihood than histories for the DROS-NOMIG model. Nevertheless, they are able to catch general history and low migration rates. Thus, based on these results it is possible to assume population isolation and use further models without migrations for more accurate estimations.

We observe interesting results for the misspecified models with structure (2, 1). In the case of the DROS-STRUCT-NOMIG model, the ground truth history of *Drosophila melanogaster* is accurately approximated by *moments* and *momentsLD* engines only. The two-epoch history of the European population is approximated by exponential growth with a rate that differs between engines (Figure S8). We note that *momentsLD* engine also is able to provide similar history for the model DROS-STRUCT-MIG with migrations. However, ∂a∂i, *momi2* and *moments* for both models are hindered by the severe local optimum and were not able to achieve a global solution within eight GADMA2 runs. The alternative history is able to catch the European population history and low migration rates, yet, it does not reflect the instantaneous expansion of the ancestral population, and the parameter value for the African population size hits the upper bound. Using models with African population size fixed to the ancestral population size after expansion helps to overcome local optimum and achieve history similar to the ground truth (section S2.1.1 of Supplementary materials, Tables S12 and S13).

Table 2. The demographic parameters of *Drosophila melanogaster* history without migration (DROS-NOMIG model) inferred with different engines in GADMA2. Ground truth are the parameter values from the paper Li and Stephan [19] used in simulation powered by *stdpopsim* [18]. Log-likelihood values are not comparable between different engines.

	Ground truth	∂a∂i	*moments*	*momi2*	*momentsLD*
Log-likelihood:		−2,808	−1,101	−53,489,812	−268
Parameters:					
N_{anc}	1,720,600	1,598,851	1,580,074	1,724,622	1,243,096
N_{AFR}	8,603,000	8,421,135	7,949,903	8,679,000	7,963,770
N_{EUP0}	2,200	21,999	16,158	439	2,013
N_{EUP}	1,075,000	1,082,115	1,008,276	1,008,970	1,102,340
T_{AFR} (gen.)	600,000	603,933	560,015	597,487	715,948
T_{split} (gen.)	158,000	173,658	162,631	159,205	153,248
T_{EUP} (gen.)	154,600	137,587	136,450	158,503	149,942

N_{anc}: size of the ancestral population; N_{AFR}: size of the African population after expansion; N_{EUP0}: European bottleneck population size after divergence; N_{EUP}: modern size of the European population; T_{AFR}: time of African size expansion; T_{split}: time of divergence; T_{EUP}: time of European expansion.

Orangutan demographic history

In the case of the orangutan simulated dataset all four engines provide similar demographic histories for the ORAN-NOMIG model without migrations. The predicted parameters are almost identical for ∂a∂i, *moments* and *momi2* which are AFS-based engines. Estimations for the modern sizes of populations are greater than the actual values used for the simulation. Moreover, the time of divergence is estimated to be lower: ~12,000 vs. ground truth of ~20,000. These discrepancies between predicted and simulated parameter values for the model ORAN-NOMIG could be explained by the fact that the model is oversimplified and lacks migration.

Model ORAN-MIG aligns correctly with the history used for data simulation. All tested engines provide estimations close to the simulated parameter values for the ORAN-MIG model.

The result demographic parameters for the ORAN-STRUCT-NOMIG model are close to the estimations obtained for the ORAN-NOMIG model. The population size dynamics are correctly inferred to be exponential for ∂a∂i and *momentsLD* engines. However, *momi2* and *moments* predict the constant size of the Bornean population. Although constant size approximates the Bornean population history relatively good, we demonstrate that our result is a consequence of the following model restriction. The model ORAN-STRUCT-NOMIG obliges the sum of Sumatran and Bornean population sizes after divergence to equal the ancestral population size. Ground truth history follows this rule, however, it is not fulfilled by the estimations inferred for the ORAN-NOMIG model. We additionally test the ORAN-NOMIG model with the same restriction on population sizes for *momi2* and *moments* engines. The best obtained scenarios have a worse log-likelihood value than histories with constant size of the Bornean population obtained for the ORAN-STRUCT-NOMIG model (section S2.2 of Supplementary materials).

The original demographic history of orangutan species used for data simulation is accurately reconstructed by ∂a∂i, *moments* and *momentsLD* engines within the ORAN-STRUCT-MIG model. Population size dynamics are inferred to be exponential for all tested engines. The parameters and values of log-likelihood are similar to the results for the ORAN-MIG model.

Table 3. The demographic parameters of orangutan history with migration for structure (1, 1) (ORAN-STRUCT-MIG model) inferred with different engines in GADMA2. Ground truth is the simulated parameter values that were obtained from the original paper Locke et al. [20]. *Momi2* engine was excluded as it does not support continuous migrations. Log-likelihood values are not comparable between different engines.

	Ground truth	∂a∂i	*moments*	*momentsLD*
Log-likelihood:		−1,220	−1,106	−53
Parameters:				
N_{anc}	17,934	17,925	17,854	17,685
N_{Bor_split}	10,617	10,432	10,498	10,529
N_{Sum_split}	7,317	7,492	7,355	7,155
N_{Bor}	8,805^{exp}	9,282^{exp}	8,892^{exp}	8,592^{exp}
N_{Sum}	37,661^{exp}	39,343^{exp}	37,443^{exp}	36,740^{exp}
$m_{Bor-Sum}(\times 10^{-5})$	0.66	0.67	0.67	0.69
$m_{Sum-Bor}(\times 10^{-5})$	1.10	1.07	1.09	1.13
T_{split} (gen.)	20,157	20,812	20,183	19,869

N_{anc}: size of the ancestral population; N_{Bor_split}: size of *Pongo pygmaeus* at split; N_{Sum_split}: size of *Pongo abelii* at split; N_{Bor}: modern size of *Pongo pygmaeus*; N_{Sum}: modern size of *Pongo abelii*; $m_{Bor-Sum}$: migration rate from *Pongo pygmaeus* to *Pongo abelii*; $m_{Sum-Bor}$: migration rate from *Pongo abelii* to *Pongo pygmaeus*; T_{split}: time of divergence.
^{exp}Exponential growth.

Table 4. The demographic parameters of orangutan histories with pulse migrations inferred using *momi2* engine in GADMA2. The time interval after divergence is divided into equal parts and pulse migrations are integrated between them. The inferred parameters show convergence to true values with an increase in pulse migration number. Ground truth is the simulated parameter values obtained from the original paper Locke et al. [20].

	Ground truth	Model ORAN-			
		NOMIG	PULSE1	PULSE3	PULSE7
Number of pulse migrations	0 (continuous)	0	1	3	7
Log-likelihood:		−48,541,453	−48,437,315	−48,391,684	−48,377,617
Parameters:					
N_{anc}	17,934	19,331	19,220	18,461	17,997
N_{Bor_split}	10,617	6,187	8,731	8,715	10,086
N_{Sum_split}	7,317	7,719	4,165	5,412	6,409
N_{Bor}	8,805	10,663	9,631	9,640	8,768
N_{Sum}	37,661	54,184	59,929	43,123	38,030
$m_{Bor-Sum}$	0.66×10^{-5}	0	0.065	0.057	0.025
$m_{Sum-Bor}$	1.10×10^{-5}	0	0.206	0.084	0.036
T_{split} (gen.)	20,157	11,270	16,211	20,086	20,809

N_{anc}: size of ancestral population; N_{Bor_split}: size of *Pongo pygmaeus* at split; N_{Sum_split}: size of *Pongo abelii* at split; N_{Bor}: size of *Pongo pygmaeus* after exponential decline; N_{Sum}: size of *Pongo abelii* after exponential size change; $m_{Bor-Sum}$: migration rate from *Pongo pygmaeus* to *Pongo abelii*; $m_{Sum-Bor}$: migration rate from *Pongo abelii* to *Pongo pygmaeus*; T_{split}: time of divergence in generations.

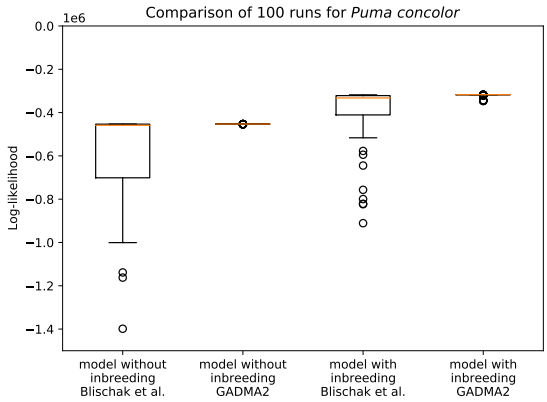

Figure 4. Boxplots for log-likelihoods obtained from 100 runs for demographic history inference of American Puma populations. Two models are used from Blischak et al. [16]: with and without inbreeding. Results from GADMA2 are compared to the results of 100 runs from the original paper by Blischak et al. [16] that were received by optimization techniques implemented in ∂a∂i. GADMA2 provides more accurate and stable solutions.

Finally, we analyze *momi2* engine performance for additional models ORAN-PULSE* with pulse events (Table 4). Inferred by *momi2* pulse migration rates differ significantly from continuous rates used in the simulation. However, they became more accurate with an increased number of pulse events. For example, the migration rate from Bornean orangutans to Sumatran orangutans ($m_{Bor-Sum}$) is inferred to be equal to 0.65 for model ORAN-PULSE1 with one pulse migration, to 0.057 for model ORAN-PULSE3 with three pulses and to 0.025 for model ORAN-PULSE7 with seven pulse events, while the continuous migration rate used in the simulation is 0.66×10^{-5} per generation. Other parameters also converge to the simulated parameter values. Along these lines, population divergence time is estimated to be ~11,000 generations for model ORAN-NOMIG, ~16,000 generations for the model ORAN-PULSE1 and ~20,000 for models ORAN-PULSE3 and ORAN-PULSE7. The latter is close to the value of 20,157 used in the simulation. Parameter estimations for model ORAN-PULSE7 with seven pulse migrations are the most accurate among tested models. We assume the increase in pulse events number will lead to more accurate estimations yet require more computational resources. Thus, continuous migration is not supported in *momi2* engine but, to some degree, could be replaced by several pulse migration events.

Usage case: inference of inbreeding coefficients

We use GADMA2 to repeat demographic inference from Blischak et al. [16] for datasets of American pumas (*Puma concolor*) and domesticated cabbage (*Brassica oleracea* var. *capitata*). Blischak et al. [16] performed the demographic inference for two models without (model 1) and with inbreeding (model 2) using ∂a∂i's optimization approaches.

First, we run GADMA2 with ∂a∂i engine and the same parameter bounds as in Blischak et al. [16] and compare the results of 100 runs with the results obtained in the original paper. The boxplots of final log-likelihood values are presented in Figure 4 for American pumas and Figure S9 for domesticated cabbage. They demonstrate that GADMA2 provides better and more stable results than usual optimization techniques from ∂a∂i within 100 runs. Several parameters of the result demographic histories for both datasets received values close to their upper or lower bounds. In order to overcome this limitation, we perform another inference with wider bounds for parameter values and observe more reliable demographic parameters.

The final values of the parameters and their confidence intervals are presented in Table S20 for American pumas and Table S21 for domesticated cabbage. The visual representations of demographic histories using *demes* can be found in Figure 5 for American pumas and in Figure 6 for domesticated cabbage.

American puma demographic history

The best demographic histories obtained with GADMA2 have better values of log-likelihood (−452,475.41 vs −453,003.05 for model 1 and −316,109.44 vs. −318,058.08 for model 2) than those reported in Blischak et al. [16]. Similar values of population sizes are obtained except for the size of the Florida population which is estimated to be 800 individuals compared to the 1,200 − 1,600 individuals estimated by Blischak et al. [16]. Time of divergence is estimated as 4,000 − 5,500 years ago. Inbreeding coefficients for model 2 are reported to be slightly higher than for the same model in Blischak et al. [16]: 0.453 for the Texas population and 0.628 for the Florida population. The Godambe-adjusted likelihood ratio statistic is 2,568.59 (P value = ~0.0; Coffman et al. [34]), indicating that the model with inbreeding better describes data.

Domesticated cabbage demographic history

The best demographic histories obtained with GADMA2 for the domesticated cabbage population have better log-likelihood values (−24137.13 vs. −24330.40 for model 1 and −4267.14 vs. −4281.14 for model 2) than those received by ∂a∂i optimization approaches. Values for the population sizes in the first and second epochs are inferred similar to the results from Blischak et al. [16]. However, the population size for the most recent epoch in our results is underestimated (6 vs 592 individuals) for model 1 without inbreeding and overestimated (174,960,000 vs. 215,000 individuals) for model 2 with inbreeding. The time duration of the epoch is also smaller

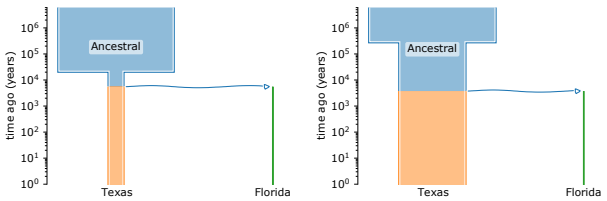

(a) Model 1 without inbreeding **(b)** Model 2 with inbreeding

Figure 5. Demographic histories for Texas and Florida populations of American puma inferred with GADMA2. Figures are generated with the *demes* package [36]. Time is presented in a log scale.

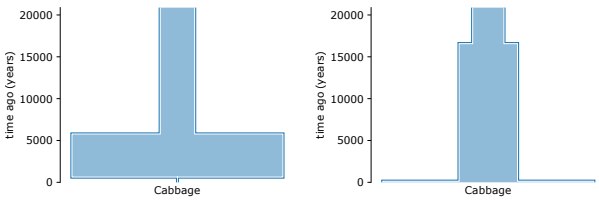

(a) Model 1 without inbreeding **(b)** Model 2 with inbreeding

Figure 6. Demographic histories for a single population of domesticated cabbage inferred with GADMA2. Figures are generated with the *demes* package. In both models, the time of the most recent epoch is estimated to be small.

for both models than estimated previously. In the case of model 1, the time parameter is very close to zero. The likelihood ratio test showed that the model with inbreeding better describes the data than the model without inbreeding (LRT statistic = 127.10, P value = ~0.0; Coffman et al. [34]).

Conclusions

GADMA2 is an extension of GADMA. It features an improved genetic algorithm, a more flexible automatic model construction setup and two additional demographic inference engines. We showcased GADMA2 by comparing different inference engines for two simulated dataset with various demographic models, including misspecified ones. Furthermore, we applied GADMA2 to infer demographic histories for two empirical datasets of inbred species, reporting updated parameters.

To improve the genetic algorithm we ran hyperparameter optimization powered by SMAC. We observed that discrete hyperparameters might hinder hyperparameter optimization, requiring much more iterations. Because of this, we manually picked five combinations of the discrete hyperparameters, running SMAC-based optimization of the remaining continuous ones for each fixed combination. We compared the set of optimal solutions on various datasets for three AFS-based inference engines of GADMA2: ∂a∂i, *moments* and *momi2*. We included the configuration that performed best when averaged across all inference engines as GADMA2's new genetic algorithm. It is worth noting, however, that different engines corresponded to different optimal configurations. We thus suggest engine-specific genetic algorithm configurations as a valuable direction for future work.

GADMA's automatic model construction setup was improved to allow forbidding specific migrations or making them symmetric, as well as restricting the admissible types of population size dynamics. Moreover, inference of selection and inbreeding coefficients was made possible in GADMA2.

Two new demographic inference engines, *momi2* and *momentsLD*, were incorporated into GADMA2. The former is based on a different mathematical model than ∂a∂i and *moments* and is computationally faster than them, but it does not support continuous migrations and linear population size growth. The latter is the first engine in GADMA2 that does not use allele frequency spectrum data for demographic inference and relies on linkage disequilibrium statistics instead. Furthermore, the new package *demes* was incorporated into GADMA2 as a representation engine providing textual and visual descriptions of demographic histories.

We analyzed the accuracy of GADMA2's demographic inference engines on two simulated datasets: the dataset of fruit fly populations and the dataset of orangutan species. We used different demographic models, including models with structures. Some of these models align with the ground truth, while some are misspecified due to various simplifications. Similar performance was observed over all engines for the models that align with the ground truth. In this case, inferred demographic histories were close to the ground truth, and the types of population size dynamics were correctly recovered for models with structures.

Demographic inference with the misspecified models demonstrated interesting phenomena. For the misspecified models with structure and the fruit fly dataset, all the AFS-based engines were stuck at the same local optimum. However, the resulting demographic histories were still able to give some insights about the studied populations. The new LD-based engine *momentsLD* performed considerably better than the AFS-based engines. For the orangutan dataset both the AFS-based engines and *momentsLD* performed well. All slight discrepancies between estimated and ground truth values are consequences of models' restrictions and misspecifications. Although the *momi2* engine does not support continuous migrations required to accurately model the ground truth, it performs well in approximating these with a number of pulse migrations. However, this approach is limited because larger numbers of pulse migrations increase computation time.

GADMA2 greatly simplifies performing such comparisons, the in-depth study of which seems a prospective work direction.

Finally, we reproduced the demographic inference setup of Blischak et al. [16] for the datasets of American pumas and domesticated cabbage, using GADMA2 with ∂a∂i engine instead of fully ∂a∂i-based inference. We demonstrated better and more stable performance of GADMA2 compared to the existing optimization techniques of ∂a∂i. We found updated parameters for models, both with and without inbreeding, from Blischak et al. [16]. For each dataset, the best demographic histories include inbreeding. Our results, however, demonstrate very broad confidence intervals for some model parameters. The wide confidence intervals for the population size of domesticated cabbage during the most recent epoch can be explained by the fact that epoch length was inferred to be small, and very recent events are difficult to investigate with the ∂a∂i engine. However, the same results for the size of the Florida puma population and the population divergence time are difficult to explain. We only tested the demographic models from Blischak et al. [16], new models, however, can be built based on our results.

GADMA2 extends the GADMA that has already shown itself as powerful and efficient software for the inference of complex demographic histories from genetic data. With its new application programming interface, GADMA2 can be easily improved further by integrating new inference engines, new optimization algorithms and automatic model construction routines.

Competing Interests

The authors declare that they have no competing interests.

Funding

This work was supported by Ministry of Science and Higher Education of the Russian Federation (Priority 2030 Federal Academic Leadership Program) [to E.N., P.D. and V.U.] and by Systems Biology Program by Skoltech [to E.N.].

References

1. Gutenkunst RN, Hernandez RD, Williamson SH, Bustamante CD. Inferring the joint demographic history of multiple populations from multidimensional SNP frequency data. PLoS genetics 2009;5(10):e1000695.
2. Jouganous J, Long W, Ragsdale AP, Gravel S. Inferring the joint demographic history of multiple populations: beyond the diffusion approximation. Genetics 2017;206(3):1549–1567.
3. Steinrücken M, Kamm J, Spence JP, Song YS. Inference of com-

plex population histories using whole-genome sequences from multiple populations. Proceedings of the National Academy of Sciences 2019;116(34):17115–17120.
4. Kamm J, Terhorst J, Durbin R, Song YS. Efficiently inferring the demographic history of many populations with allele count data. Journal of the American Statistical Association 2020;115(531):1472–1487.
5. Excofffier L, Marchi N, Marques DA, Matthey-Doret R, Gouy A, Sousa VC. fastsimcoal2: demographic inference under complex evolutionary scenarios. Bioinformatics 2021;.
6. DeWitt WS, Harris KD, Ragsdale AP, Harris K. Nonparametric coalescent inference of mutation spectrum history and demography. Proceedings of the National Academy of Sciences 2021;118(21).
7. Ragsdale AP, Gutenkunst RN. Inferring demographic history using two-locus statistics. Genetics 2017;206(2):1037–1048.
8. Ragsdale AP, Gravel S. Models of archaic admixture and recent history from two-locus statistics. PLoS genetics 2019;15(6):e1008204.
9. Ragsdale AP, Gravel S. Unbiased estimation of linkage disequilibrium from unphased data. Molecular Biology and Evolution 2020;37(3):923–932.
10. Noskova E, Ulyantsev V, Koepfli KP, O'Brien SJ, Dobrynin P. GADMA: Genetic algorithm for inferring demographic history of multiple populations from allele frequency spectrum data. GigaScience 2020;9(3):giaa005.
11. Xiong P, Hulsey CD, Fruciano C, Wong WY, Nater A, Kautt AF, et al. The comparative genomic landscape of adaptive radiation in crater lake cichlid fishes. Molecular ecology 2021;30(4):955–972.
12. Valdez L, D'Elía G. Genetic Diversity and Demographic History of the Shaggy Soft-Haired Mouse Abrothrix hirta (Cricetidae; Abrotrichini). Frontiers in Genetics 2021;12:184.
13. Pazhenkova EA, Lukhtanov VA. Genomic introgression from a distant congener in the Levant fritillary butterfly, Melitaea acentria. Molecular Ecology 2021;.
14. Cassin-Sackett L, Campana MG, McInerney NR, Lim HC, Przelomska NA, Masuda B, et al. Genetic structure and population history in two critically endangered Kaua 'i honeycreepers. Conservation Genetics 2021;p. 1–14.
15. Buggiotti L, Yurchenko AA, Yudin NS, Vander Jagt CJ, Vorobieva NV, Kusliy MA, et al. Demographic history, adaptation, and NRAP convergent evolution at amino acid residue 100 in the world northernmost cattle from Siberia. Molecular Biology and Evolution 2021;.
16. Blischak PD, Barker MS, Gutenkunst RN. Inferring the demographic history of inbred species from genome-wide SNP frequency data. Molecular biology and evolution 2020;37(7):2124–2136.
17. Gutenkunst RN. dadi. CUDA: Accelerating population genetics inference with graphics processing units. Molecular biology and evolution 2021;38(5):2177–2178.
18. Adrion JR, Cole CB, Dukler N, Galloway JG, Gladstein AL, Gower G, et al. A community-maintained standard library of population genetic models. Elife 2020;9.
19. Li H, Stephan W. Inferring the demographic history and rate of adaptive substitution in Drosophila. PLoS genetics 2006;2(10):e166.
20. Locke DP, Hillier LW, Warren WC, Worley KC, Nazareth LV, Muzny DM, et al. Comparative and demographic analysis of orang-utan genomes. Nature 2011;469(7331):529–533.
21. Kelleher J, Etheridge AM, McVean G. Efficient coalescent simulation and genealogical analysis for large sample sizes. PLoS computational biology 2016;12(5):e1004842.
22. Schrider DR, Houle D, Lynch M, Hahn MW. Rates and genomic consequences of spontaneous mutational events in Drosophila melanogaster. Genetics 2013;194(4):937–954.
23. Comeron JM, Ratnappan R, Bailin S. The Many Landscapes of Recombination in Drosophila melanogaster. PLOS Genetics 2012 10;8(10):1–21. https://doi.org/10.1371/journal.pgen.1002905.
24. Nater A, Mattle-Greminger MP, Nurcahyo A, Nowak MG, De Manuel M, Desai T, et al. Morphometric, behavioral, and genomic evidence for a new orangutan species. Current Biology 2017;27(22):3487–3498.
25. Ochoa A, Onorato DP, Fitak RR, Roelke-Parker ME, Culver M. De novo assembly and annotation from parental and F1 puma genomes of the Florida panther genetic restoration program. G3: Genes, Genomes, Genetics 2019;9(11):3531–3536.
26. Cheng F, Wu J, Cai C, Fu L, Liang J, Borm T, et al., Genome resequencing and comparative variome analysis in a Brassica rapa and Brassica oleracea collection. Sci Data 3: 160119; 2016.
27. Cheng F, Sun R, Hou X, Zheng H, Zhang F, Zhang Y, et al. Subgenome parallel selection is associated with morphotype diversification and convergent crop domestication in Brassica rapa and Brassica oleracea. Nature genetics 2016;48(10):1218–1224.
28. Snoek J, Larochelle H, Adams RP. Practical bayesian optimization of machine learning algorithms. Advances in neural information processing systems 2012;25.
29. Hutter F, Hoos HH, Leyton-Brown K. Sequential model-based optimization for general algorithm configuration. In: International conference on learning and intelligent optimization Springer; 2011. p. 507–523.
30. Lindauer M, Eggensperger K, Feurer M, Biedenkapp A, Deng D, Benjamins C, et al. SMAC3: A Versatile Bayesian Optimization Package for Hyperparameter Optimization. Journal of Machine Learning Research 2022;23(54):1–9. http://jmlr.org/papers/v23/21-0888.html.
31. Lago J, De Ridder F, Vrancx P, De Schutter B. Forecasting day-ahead electricity prices in Europe: The importance of considering market integration. Applied energy 2018;211:890–903.
32. Hewamalage H, Bergmeir C, Bandara K. Recurrent neural networks for time series forecasting: Current status and future directions. International Journal of Forecasting 2021;37(1):388–427.
33. Wu S, Song X, Feng Z, Wu X. NFLAT: Non-Flat-Lattice Transformer for Chinese Named Entity Recognition. arXiv preprint arXiv:220505832 2022;.
34. Coffman AJ, Hsieh PH, Gravel S, Gutenkunst RN. Computationally efficient composite likelihood statistics for demographic inference. Molecular biology and evolution 2016;33(2):591–593.
35. Myers S, Fefferman C, Patterson N. Can one learn history from the allelic spectrum? Theoretical population biology 2008;73(3):342–348.
36. Gower GR, Ragsdale AP, Gutenkunst RN, Hartfield M, Noskova E, Struck TJ, et al. Demes: a standard format for demographic models. bioRxiv 2022;.
37. Rosenbrock H. An automatic method for finding the greatest or least value of a function. The computer journal 1960;3(3):175–184.